Journal of Multidisciplinary Engineering Science and Technology (JMEST)
ISSN: 3159-0040
Vol. 2 Issue 8, August - 2015

Active Vibration Control Of Pipes Conveying Fluid Using Piezoelectric Actuators

[1]Prof.Dr. Muhsin J.Jweeg , [2*]Thaier J.Ntayeesh
[1] Mechanical Engineering Department, AL_Nahrain University,Baghdad,Iraq
[2] Mechanical Engineering Department, University of Baghdad,Baghdad,Iraq
[*] Correspondence: Thaier_aljabbery@yahoo.com

***Abstract*— This paper deal with the problem about active control of parametric resonance of pinned-pinned pipes conveying . the active controllers are designed in view of the parametric resonance. Piezoelectric ceramics are used as actuators and mode transducer in control.**

The core part of the paper is the design of controllers. First, on the basis of linear quadratic optimal control theory, the optimal controller is designed in accordance with the linear time invariant part of the system, because the stabilities of the pipes are mainly determined by their linear part and the speed of fluid varies in small range. Second, on the basis of optimal controller.

The validity of controllers is examined by numerical simulation. The result of the numerical simulation states that every controller has its characteristic respectively and is very effective to control the parametric resonance of the pipes and to resist parametric turbulence. In addition, the impact of the system parameters on performance of the controllers is discussed in this paper.

Keywords— Smart structure, Pipe conveying fluid, Active control, Piezoelectric Actuator.

1.INTRODUCTION .

Pipes conveying flow, a flow conveying carrier, has widely applied for those engineering field which contains fuel supply pipes of Aerospace engines, inflow pipes of hydro turbine, and oil conveying flow of petrochemical enterprise. In addition, various type of pipes are generally utilized in large scale vehicles and constructional engineering. The proposed research indicates that fluid action could result in severe vibration of pipes system after disturbance. The vibrations could cause noise, pipeline breaks and fluid leakage when the vibration strength reaches a certain level and last longer. Therefore, the overseas studies have paid attention to the issue of pipes vibration control with effective active control methods.

The structure which contains mass and elasticity could generate vibration easily during movements. For the sake of these issues, designers have composed many methods. Firstly, let inherent frequency away from excitation frequency, which makes inherent frequency calculation become core calculation content on early vibration analyses. Secondly, some vibration absorption and isolation devices are added on the structure. For instance, additional elastic damper installed on bridge, high tension cable, and high buildings; rotary vacuum cleaner installed on diesel engine principal axis; spring added between car wheels and body; elastic gasket used during instruments transportation. These devices use the combination effects of additional mass, spring or damper to absorb or isolate system vibrations without extra energy, which calls passive absorber. It is still a practical and effective vibration attenuation method at present, because it could restrains system narrow band vibration primly. While, with the development of novel technologies, a new type of vibration appeals which contains low inherent frequency and wide frequency domain. For this type of vibration, passive vibration damping is not applicable. Therefore, a navel control method called active control which integrates external energy as control force to restrain system vibration has been developed rapidly and widely utilized in several domains. To compare with passive control, active control has better flexibility and environmental adaptability, also can effectively control extra low frequency vibration and wide frequency vibration. Recently, the main adopted active control strategies include pole assignment control, optimal control, self-adaptation control, fuzzy control, and artificial neural network control et.al.

At present, a large number of articles at home and abroad focus on pipes conveying fluid and flexible beam structure vibration control field. For example, [1]and [2] introduced independent mode space concept in optimal control and model reference self-adaptation control, and adopt ceramic piezoelectric sheets as simulator to control cantilever pipes conveying fluid vibration under steady flow. [3] Conducted active control on nonlinear restrains cantilever pipes conveying fluid vibration under steady flow with ceramic piezoelectric sheets as simulator. [4] Conducted active control on fixed at both ends of pipes vibration under over critical velocity steady flow based on optimal independent mode space control method with ceramic piezoelectric sheets as simulator. [5] studied cantilever pipes conveying fluid vibration control under steady flow, and flexible cantilever beam vibration control. All of above articles used ceramic piezoelectric sheets as simulator. These articles showed ceramic piezoelectric sheets have been widely applied for control simulator and mode sensor design. Using ceramic piezoelectric sheets as mode sensor takes the advantage of direct piezoelectric effects of piezoelectric ceramic. Direct

piezoelectric effects refer to some mediums deformations under force due to lack of symmetric centre, and caused surface electrification. On the contrary, adding exciting electric field will cause mechanical deformations, which calls inverse piezoelectric effects. Based on this feature, ceramic piezoelectric sheets are designed as simulator. [6][7][8][9][10] Implemented active control for different system vibration problems via ceramic piezoelectric sheets.The most popular and dangerous vibration in engineering field is pulsating flow caused motions. Normally, pipes flow are supported by forcing from compressor or pump, while, due to the intermittent of this method, fluid will generate pulsating pressure, and forms pulsating flow. Research indicated that pinned both ends of pipes could lose stability caused by parameter resonance. Most of existing articles focused on pipes conveying fluid vibration control problem under steady flow. The pipes vibration control problems are still open. Therefore, the proposed research will focus on active control problems of pinned at both ends of pipes conveying fluid vibrations.

2.SYSTEM DYNAMIC

The equation of motion for the transverse vibration of the pipe is given as:Maintaining the Integrity of the Specifications:

$$\left(1+a\frac{\partial}{\partial t}\right)EI\frac{\partial^4 y}{\partial x^4}+\{MU^2-\overline{T}+A\bar{P}(1-2v\delta)-[(M+m)g-M\dot{U}](L-x)\}\frac{\partial^2 y}{\partial x^2}-\left[\left(1+a\frac{\partial}{\partial t}\right)\frac{E\tilde{A}}{2L}\int_0^L (y')^2\,dx\right]\frac{\partial^2 y}{\partial x^2}+(M+m)\frac{\partial^2 y}{\partial t^2}+2MU\frac{\partial^2 y}{\partial x\partial t}+(M+m)g\frac{\partial y}{\partial x}=0 \quad (2.1)$$

The material of pipes is viscoelastic, and corresponds with Kelvin-Voigt assumption which stress-strain satisfies:

$$\sigma=\left(1+a\,\frac{\partial}{\partial a}\right)E\varepsilon$$

M- fluid mass per unit length, U-fluid velocity, P-per unit area fluid pressure, A- flow cross section area
Q- shear force on pipe unit cross section; T- axial force on pipe unit cross section; m- per unit length pipe mass. In order to obtain generalized motion differential equation, and avoid unit effects, the dimensionless is necessary for motion equation (2.15). Meantime, in order to simplify analyzing questions, dimensionless parameter is introduced and conducts changes to transform partial differential equation (2.15) into dimensionless differential equation. Dimensionless parameters are:

$$\eta=\frac{y}{L}\ ,\ \xi=\frac{x}{L}\ ,\ \bar{g}=\frac{M+m}{EI}L^3 g\ ,$$
$$\tau=\left(\frac{EI}{M+m}\right)^{\frac{1}{2}}\frac{t}{L^2}\ ,\ \Gamma=\frac{\overline{T}L^2}{EI},\Pi=\frac{\bar{P}AL^2}{EI}$$
$$\gamma=\frac{\tilde{A}L^2}{2I},u=\left(\frac{M}{EI}\right)^{\frac{1}{2}}LU\ ,\ M_r=\left(\frac{M}{M+m}\right)^{\frac{1}{2}},$$
$$\alpha=\left(\frac{EI}{M+m}\right)^{\frac{1}{2}}\frac{a}{L^2} \quad (2.2)$$

Plugging (2.2) into (2.1), the dimensionless differential equation is found:

$$\eta^{(4)}+\alpha\dot{\eta}^{(4)}+\Big[u^2-\Gamma+\Pi(1-2v\delta)+(M_r\dot{u}-\overline{g})(1-\xi)\quad-\gamma\int_0^1(\eta')^2\,d\xi-2\alpha\gamma\int_0^1\eta'\dot{\eta}'d\xi\Big]\eta''+\ddot{\eta}+2M_r u\dot{\eta}'+\bar{g}\eta'=0 \quad (2.3)$$

In the equation, $(\ )'$ refers $\frac{\partial(\ )}{\partial\xi}$, $(\dot{})$ refers $\frac{\partial(\ )}{\partial\tau}$.
Placing nonlinear part on the right side of equation, the dimensionless equation then is found:

$$\ddot{\eta}+2M_r u_0\dot{\eta}'+\alpha\dot{\eta}^{(4)}+\eta^{(4)}+[{u_0}^2-\Gamma+\Pi(1-2v\delta)-\bar{g}]\eta''+\bar{g}\xi\eta''+\bar{g}\eta' = +2\alpha\gamma\eta''\int_0^1\eta'\dot{\eta}'d\xi+\gamma\eta''\int_0^1(\eta')^2\,d\xi \quad (2.4)$$

In order to simplify the analyses of motion differential equation, the dimensionless high order differential equation (2.4) is discretized and decrease order to a lower order differential equation via Ritz-Galerkin method. Supposing displacement η as a function of variables ξ and τ, and its Ritz-Galerkin expression will be:

$$\eta(\xi,\tau)=\sum_{i=1}^{\infty}\phi_i(\xi)q_i(\tau) \quad (2.5)$$

$q_i(\tau)$ is an generalized coordinate, $\phi_i(\xi)$ is an comparison function which satisfies all the boundary conditions. Selecting the first two orders conducts researches, which is:

$$\eta(\xi,\tau)=\sum_{i=1}^{2}\phi_i(\xi)q_i(\tau)=\phi_1(\xi)q_1(\tau)+\phi_2(\xi)q_2(\tau) \quad (2.6)$$

For pined at both ends of pipes, its vibration model function is:

$$\phi_i=\sqrt{2}\,sin(\lambda_i\xi),\ i=1,2 \quad (2.7)$$

$\lambda1$ and $\lambda2$ are pipe's eigenvalues, $\lambda1=\pi,\lambda2=2\pi$ are for pinned at both ends of pipes (2.6) is changed into matrix type, supposing $\Phi=\begin{Bmatrix}\phi_1\\ \phi_2\end{Bmatrix}$, $Q=\begin{Bmatrix}q_1\\ q_2\end{Bmatrix}$, then

$$\eta(\xi,\tau)=\Phi^T Q=Q^T\Phi$$

Plugging (2.6) into (2.19), and supposing

$$T=\Gamma-\Pi(1-2v\delta),\ \text{then:}$$

$$\phi^T\ddot{Q}+2M_r u_0\phi'^T\dot{Q}+\alpha\phi^{(4)T}\dot{Q}+({u_0}^2-T-\bar{g})\phi''^T Q+\bar{g}\xi\phi''^T Q+\bar{g}\phi'^T Q\quad+\phi^{(4)T}Q= +2\alpha\gamma\int_0^1 Q^T\phi'\phi'^T\dot{Q}\,d\xi\phi''^T Q+\gamma\int_0^1 Q^T\phi'\phi'^T Q d\xi\phi''^T Q \quad (2.9)$$

By multiplying $\Phi=\begin{Bmatrix}\phi_1\\ \phi_2\end{Bmatrix}$ with two sides of (2.9) and

then transform it into below type:

$$\Phi\Phi^T\ddot{Q}+2M_r u_0\Phi\Phi'^T\dot{Q}+\alpha\Phi\Phi^{(4)T}\dot{Q}+({u_0}^2-T-\bar{g})\Phi\Phi''^T Q+\bar{g}\xi\Phi\Phi''^T Q+\bar{g}\Phi\Phi'^T Q+\Phi\Phi^{(4)T}Q= 2\alpha\gamma\int_0^1 Q^T\Phi'\Phi''^T\dot{Q}\,d\xi\Phi\Phi''^T Q+\gamma Q^T\int_0^1\Phi'\Phi'^T Q d\xi\Phi\Phi''^T Q \quad (2.10)$$

Conducting ξ integral to (2.10) at interval [0, 1], and substitutions based on orthogonality of trigonometric function:

$\int_0^1 \phi\phi^T d\xi = I\,, \quad \int_0^1 \phi\phi'^T d\xi = B\,, \int_0^1 \phi'\phi'^T d\xi = -C,$
$\int_0^1 \phi\phi''^T d\xi = C$

$$\int_0^1 \xi\phi\phi''^T d\xi = D \ \int_0^1 \phi\phi^{(4)T} d\xi = \Lambda = \begin{pmatrix} {\lambda_1}^4 & \\ & {\lambda_2}^4 \end{pmatrix} \quad (2.11)$$

Using equations of (2.11), the discretized equation after reduced order through (2.10) is showed below:

$$I\ddot{Q} + 2M_r u_0 B\dot{Q} + ({u_0}^2 - T - \bar{g})CQ + \alpha\Lambda\dot{Q} + \bar{g}DQ + \bar{g}BQ + \Lambda Q = -2\alpha\gamma Q^T C\dot{Q}CQ - \gamma Q^T CQCQ \quad (2.12)$$

Supposing E=B+D-C, then (2.12) will be further transformed into:

$$I\ddot{Q} + (2M_r u_0 B + \alpha\Lambda)\dot{Q} + [({u_0}^2 - T)C + \Lambda]Q + \alpha\Lambda\dot{Q} + \bar{g}EQ = -2\alpha\gamma Q^T C\dot{Q}CQ - \gamma Q^T CQCQ \quad (2.13)$$

In the equation,

$$B = \begin{pmatrix} 0 & -b \\ b & 0 \end{pmatrix}, \quad C = \begin{pmatrix} c_{11} & -b \\ b & c_{22} \end{pmatrix},$$
$$E = \begin{pmatrix} -\frac{1}{2}c_{11} & e \\ e & -\frac{1}{2}c_{22} \end{pmatrix}$$

For pinned at both ends of pipes, it is calculated that:

$$b = \frac{8}{3}\,, \quad c_{11} = -\pi^2\,, \quad c_{22} = -4\pi^2\,, \quad e = \frac{40}{9} \quad (2.15)$$

Plugging (2.15) into (2.13), after arrangements:

$$\begin{pmatrix} \ddot{q}_1 \\ \ddot{q}_2 \end{pmatrix} + \begin{pmatrix} \alpha{\lambda_1}^4 & -2M_r u_0 b \\ 2M_r u_0 b & \alpha{\lambda_2}^4 \end{pmatrix} \begin{pmatrix} \dot{q}_1 \\ \dot{q}_2 \end{pmatrix} + \begin{pmatrix} \left({u_0}^2 - T - \frac{1}{2}\bar{g}\right)c_{11} + {\lambda_1}^4 & \bar{g}e \\ \bar{g}e & \left({u_0}^2 - T - \frac{1}{2}\bar{g}\right)c_{22} + {\lambda_2}^4 \end{pmatrix}$$

$$\begin{pmatrix} q_1 \\ q_2 \end{pmatrix} = - \begin{pmatrix} Q_1 \\ Q_2 \end{pmatrix} \quad (2.16)$$

Q refer to pulsating nonlinear part, the specific expressions is:

$$\begin{pmatrix} Q_1 \\ Q_2 \end{pmatrix} = 2\alpha\gamma \begin{pmatrix} q_1 & q_2 \end{pmatrix} \begin{pmatrix} c_{11} & 0 \\ 0 & c_{22} \end{pmatrix} \begin{pmatrix} \dot{q}_1 \\ \dot{q}_2 \end{pmatrix}$$

$$\begin{pmatrix} c_{11} & 0 \\ 0 & c_{22} \end{pmatrix} \begin{pmatrix} q_1 \\ q_2 \end{pmatrix} + \gamma \begin{pmatrix} q_1 & q_2 \end{pmatrix} \begin{pmatrix} c_{11} & 0 \\ 0 & c_{22} \end{pmatrix} \begin{pmatrix} q_1 \\ q_2 \end{pmatrix} \begin{pmatrix} c_{11} & 0 \\ 0 & c_{22} \end{pmatrix} \begin{pmatrix} q_1 \\ q_2 \end{pmatrix} \quad (2.17)$$

Suppose,

$$a_1 = -\left({u_0}^2 - T - \frac{1}{2}\bar{g}\right)c_{11} + {\lambda_1}^4$$

$$a_2 = -\bar{g}e\,, \quad a_3 = -\alpha{\lambda_1}^4, \quad a_4 = 2M_r u_0 b$$

$$b_2 == -\left({u_0}^2 - T - \frac{1}{2}\bar{g}\right)c_{22} + {\lambda_2}^4$$

$$b_4 = -\alpha{\lambda_2}^4$$

and $$\begin{pmatrix} x_1 \\ x_2 \\ x_3 \\ x_3 \end{pmatrix} = \begin{pmatrix} q_1 \\ q_2 \\ \dot{q}_1 \\ \dot{q}_2 \end{pmatrix} \quad (2.18)$$

Thus, (2.13) can be change into first mode state differential equation, which is:

$$\begin{pmatrix} x_1 \\ x_2 \\ x_3 \\ x_3 \end{pmatrix} = \begin{pmatrix} 0 & 0 & 1 & 0 \\ 0 & 0 & 0 & 1 \\ a_1 & a_2 & a_3 & a_4 \\ a_2 & b_2 & -a_4 & b_4 \end{pmatrix} + - \begin{pmatrix} 0 \\ 0 \\ Q_1 \\ Q_2 \end{pmatrix} \quad (2.19)$$

The system motion response simulation will base on this equation.

3.SYSTEM DYNAMIC

The pure linear control system is not exist because it is more or less nonlinear in real control system, while under certain conditions, it has not significant errors if some systems are managed with linear methods. The linear control system design is applicable for real projects. In this chapter, ceramics piezoelectric sheets are applied for designing control actuators. Controlled system functions are attained by adding control torque generated from piezoelectric sheets stretch of the original uncontrolled system. Based on the optimal control theories of second mode performance index, the optimal controller is designed aimed at the linear time-invariant of controlled system. Finally, date simulation methods are applied for evaluate the validation of controller.

3.1Controlled system equations of motion

Figure 3.1 shows the controlled system model of pipes conveying fluid.

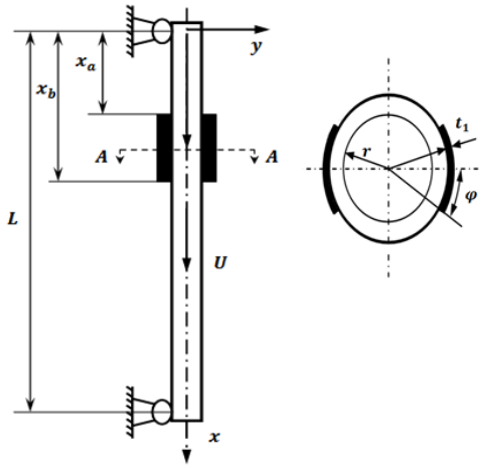

Figure 3.1pinned at both ends of pipes conveying fluid model

Two piezoelectric sheets are sticked symmetrically on the left and right side of pipes, and located on the same layer with pipes axis. x_a and x_b are the distances of both ends of piezoelectric sheets and the top of pipes respectively. Due to the stretches of piezoelectric sheets, pipes will be influenced by torque when applying voltage at two sides of piezoelectric sheets simultaneously. Torque equation is shown below:

$$M_f = \frac{4\psi E_A d_a[(r+t_1)^3 - r^3]sin\varphi}{3(1+\psi)t_1} V = C_m V \quad (3.1)$$

EI and $E_A I_A$ are the flexural stiffness of pipes and piezoelectric sheets respectively. r is outside diameter. d_a is piezoelectric constant .t_1 is the thickness of piezoelectric sheets. φ is the half angle envelop of piezoelectric sheets. V is controlled input voltage. The controlled system nonlinear equation of motion is generated by adding control torque into uncontrolled pipes equation of motion:

$$\left(1 + a\frac{\partial}{\partial t}\right) EI \frac{\partial^4 y}{\partial x^4} + \{MU^2 - \overline{T} + \bar{P}A(1-2v\delta) - [(M+m)g - M\dot{U}](L-x)\}\frac{\partial^2 y}{\partial x^2} - \left[\left(1 + a\frac{\partial}{\partial t}\right)\frac{E\tilde{A}}{2L}\int_0^L (y')^2\,dx\right]\frac{\partial^2 y}{\partial x^2} + (M+m)g\frac{\partial y}{\partial x} = \frac{\partial}{\partial x}\{C_m V[\delta(x,x_a) - \delta(x,x_b)]\} \quad (3.2)$$

δ is Dirac delta function.

Based on Eq. (2.2), dimensionless variables are defined as follows:

$$\xi_a = \frac{x_a}{L} \qquad \xi_b = \frac{x_b}{L} \qquad v = \frac{LC_m}{EI} V \quad (3.3)$$

Same method as section 2 is adopted for dimensionless Eq. (3.2). It is attained by discretization using Galerkin Function.

$$\dot{X} = AX + Bv + F(X,\tau) \quad (3.4)$$

Where

$$X = (x_1, x_2, x_3, x_4)^T,\ B = (0,0,B_3,B_4)^T$$
$$F(X,\tau) = (0,0,-Q_1,-Q_2)$$

$$A = \begin{pmatrix} 0 & 0 & 1 & 0 \\ 0 & 0 & 0 & 1 \\ a_1 & a_2 & a_3 & a_4 \\ a_2 & b_2 & -a_4 & b_4 \end{pmatrix}$$

$$B_3 = \varphi_1'(\xi_b) - \varphi_1'(\xi_a),\ B_4 = \varphi_2'(\xi_b) - \varphi_2'(\xi_a)$$

In this equation, The expression of $a_i\ (i = 1,2,3,4)$, $b_i (i = 2,4)$, $Q_i\ (i = 1,2)$ are equivalent to Eq. (2.18).

3.2 Optimal controller design

The proposed research of pipes conveying fluid pulsating flow is a time-varying nonlinear system. Because it has small disturbance in real objects, thus, the system stability is determined by the linear parts. Furthermore, it also shows small time-varying range of system parameters. Hence, the controller is able to be designed according to the system linear time-invariant, and following an evaluation of control effects of system vibrations.

The linear time-invariant of Eq.(3.4) is

$$\dot{X} = AX + Bv \quad (3.5)$$

System output variables is displacement of the top of pipes, which is

$$y = \eta(\xi) = CX \quad (3.6)$$

Where $C = [\varphi_1(\xi), \varphi_2(\xi), 0, 0]$

Equation of state of linear time-invariant system is

$$\begin{cases} \dot{X} = AX + Bv \\ y = CX \end{cases} \quad (3.7)$$

Supposing the second objective function is

$$J = \int_0^\infty (X^T QX + v^T Rv)dt \quad (3.8)$$

In this equation, Q is a positive definite or semidefinite symmetric real matrix. R is positive number. The first integral of objective function J trends toward a minimum. It means that the system requires a minimum accumulated error while state variables away from equilibrium point. When the second integral reaches a minimum represents that the consumed control energy is a minimum during the control process. Q and R are weight matrix and weight coefficient which are used to determine the ratio of state variables and control variables in the performance index. It is concluded that the control inputs are relevant to Q and R.

The aim of second mode optimal control is searching the law v of optimal control that make a minimum of second mode objective function J. The law of optimal control can be inferred through principle of minimum with Hamiltonian function.

$$H(X,\lambda,t) = \frac{1}{2}(X^T QX + v^T Rv) + \lambda^T(AX + Bv) \quad (3.9)$$

Principle of minimum requires optimal control and state variation locus to satisfy below three equations, which is

$$\begin{cases} \dot{X} = \frac{\partial H}{\partial \lambda} & X(0) = X_O \\ -\dot{\lambda} = \frac{\partial H}{\partial X} & \\ \frac{\partial H}{\partial v} = 0 & \lambda(T) = 0 \end{cases} \quad (3.10)$$

Through matrix and differential of vector, Eq. (3.11) can be changed to

$$\begin{cases} \dot{X} = AX + Bv & X(0) = X_O \\ -\dot{\lambda} = QX + A^T\lambda & \\ v^* = -R^{-1}B^T\lambda & \lambda(T) = 0 \end{cases} \quad (3.11)$$

In above Equations, v is the optimal control input when integral final value time is T in J. For reaching optimal control via linear response method, it is generally expected that λ is represented as linear function of X.

$$\lambda = PX \quad (3.12)$$

Conducting differential on both side, and plugging (3.10) and (3.11)

$$\dot{P} + PA - PR^{-1}B^TP = -Q - A^TP \quad (3.13)$$

Above is Riccati equation. when T→∞, it is reduced to

$$A^TP + PA - PR^{-1}B^TP + Q = 0 \quad (3.14)$$

The solution of equation P is positive definite constant matrix. Plugging Eq. (3.12) into v of Eq. (3.9), then the optimal control inputs is

$$v = v^* = -R^{-1}B^TPX \quad (3.15)$$

Supposing linear response matrix is

$$K = -R^{-1}B^TP \quad (3.16)$$

Optimal control input can be wrote as

$$v = -KX \quad (3.17)$$

It is certified by Lyapunov theorem that current linear control system is asymptotic stability. By taking Lyapunov function S

$$S = X^TPX \quad (3.18)$$

Taking the derivative of Eq. (3.18)

$$\dot{S} = \frac{d}{dt}(X^TPX) = \dot{X}^TPX + X^TPX = (AX + Bv)^TPX + X^TP(AX + Bv) \quad (3.19)$$

Plugging Eq. (3.14) and Eq. (3.15) into above equation,

$$\dot{S} = -X^TPBR^{-1}B^TPX - X^TQX \quad (3.20)$$

Modifying Eq. (3.2) and then plugging Eq.(3.15) into this equation,

$$\dot{S} = -(v^TRv + X^TQX) \quad (3.21)$$

When R and Q are positive definite, S is negative definite. It can be seen that the system is asymptotic stability. After control input expression of system is established, the optimal value of relevant parameters is further conducted, which can be found from Eq. (3.19) and Eq. (3.21).

$$\frac{d}{dt}(X^TPX) = -(v^TRv + X^TQX) \quad (3.22)$$

Therefore, objective function,

$$J = -\int_0^\infty \frac{d}{dt}(X^TPX)dt = -X^T(\infty)PX(\infty) + X^T(0)PX(0) \quad (3.23)$$

Where $\to \infty$, $X(\infty) \to 0$, $J = X^T(0)PX(0)$ (3.24)

In data simulation, above equation will be applied for understanding the impacts of piezoelectric sheets length and position on system control effects.

3.3 Mode sensor design

For controller based positive control system, it is necessary to calculate the state variables of system thereby obtaining system control inputs. In general, there are two methods to get the state variables of system, which includes using state viewer and mode sensor. State viewer that is rely on the system output refactors state variables of system through nominal model, but it is only applicable for linear system. Therefor, in this section, a method which using positive piezoelectric effects of ceramics piezoelectric sheets described in [28] is adopted to design mode sensor. The positive piezoelectric effect refers to some mediums which will cause deformations under the action of force duo to lack of symmetric center inside, and it arouse medium surface with an electrical charge. On the contrary, applying excitation electric field, medium to generate mechanical deformation, called the inverse piezoelectric effect.

Because of the features of the inverse piezoelectric effect, ceramic piezoelectric sheets are applicable as control actuators. In this proposed system, two ceramic piezoelectric sheets are placed on the pipe's surface as sensor, because system requires the first two mode weights. Piezoelectric sheets width is b. Piezoelectric constant is d_a. Length are L_1 and L_2 respectively. Then the output quality of electric charge of piezoelectric sheets is

$$W_i(\tau) = bd_a \int_{L_i} \varepsilon_i(\xi, \tau)d\xi \ , \ (i = 1,2) \quad (3.25)$$

In this equation, integrating range is dimensionless length range of piezoelectric sheets. $\varepsilon(\xi, \tau)$ is piezoelectric sheets strain,

$$\varepsilon_i(\xi, \tau) = -y_i\eta''(\xi, \tau) \quad (3.26)$$

y_i is y coordinate of piezoelectric sheets middle-level. Making first order derivative for time in Eq. (3.25), the output electricity is:

$$I_i = bd_a \int_{L_i} \dot{\varepsilon}_i(\xi,\tau)d\xi \qquad (3.27)$$

According to the Ritz-Galerkin equation in last chapter, mode truncation equation is acquired as follows:

$$\eta(\xi,\tau) = \sum_{j=1}^{\infty} \phi_j(\xi)X_j\,, \quad (j = 1,2) \qquad (3.28)$$

Plugging Eq.(3.27) and Eq.(3.29) into Eq.(3.26),

$$W_i(\tau) = bd_a \sum_{j=1}^{2}\left[\int_{Li} y_i\phi_j''(\xi)d\xi\right]x_j\,, \quad (j = 1,2) \qquad (3.29)$$

It also can be wrote in matrix, which is:

$$\begin{bmatrix} W_1(\tau) \\ W_2(\tau) \end{bmatrix} = -bd_a\varepsilon \begin{bmatrix} x_1 \\ x_2 \end{bmatrix} \qquad (3.30)$$

Where

$$\varepsilon = \begin{bmatrix} \varepsilon_{11} & \varepsilon_{12} \\ \varepsilon_{21} & \varepsilon_{22} \end{bmatrix}, \varepsilon_{ij} = \int_{Li} y_i\phi_j''(\xi)d\xi\ , (i,j = 1,2) \qquad (3.31)$$

Non-singular matrix ε can be generated by placing the position of sensor appropriately, and mode displacement value is defined below:

$$\begin{bmatrix} x_1 \\ x_2 \end{bmatrix} = -\frac{1}{bd_a}\varepsilon^{-1}W \qquad (3.32)$$

Mode speed value is calculated by making derivation of time in above equation:

$$\begin{bmatrix} x_3 \\ x_4 \end{bmatrix} = \begin{bmatrix} \dot{x}_1 \\ \dot{x}_2 \end{bmatrix} = -\frac{1}{bd_a}\varepsilon^{-1}I \qquad (3.33)$$

It is emphasized that in above mentioned closed-loop system, mode displacement and speed from mode sensor are observed value rather then real value. There are some higher modes which are not taken into account, because in real project, it will be filtered by mode filter.

4.Numerical Simulation

In order to test the result of former designed controller, Numerical Simulation is developed in this section.

Eq. (3.15) and (3.17) are substituted to (3.4), then the original controlled system can be described as following:

$$\dot{X} = (A - R^{-1}BB^TP)X + F(X,\tau) = A_cX + F(X,\tau) \qquad (3.34)$$

Among these,

$$A_c = \begin{pmatrix} 0 & 0 & 1 & 0 \\ 0 & 0 & 0 & 1 \\ a_{c1} & a_{c2} & a_{c3} & a_{c4} \\ a_{c2} & b_{c2} & -a_{c4} & b_{c4} \end{pmatrix}, P = \begin{pmatrix} P_{11} & P_{12} & P_{13} & P_{14} \\ P_{21} & P_{22} & P_{23} & P_{24} \\ P_{31} & P_{32} & P_{33} & P_{34} \\ P_{41} & P_{42} & P_{43} & P_{44} \end{pmatrix}$$

$$a_{c1} = a_1 - R^{-1}B_3(B_3P_{31} + B_4P_{41})\,, a_{c2} = a_2 - R^{-1}B_3(B_3P_{32} + B_4P_{42})$$

$$a_{c3} = a_3 - R^{-1}B_3(B_3P_{33} + B_4P_{43})\,, a_{c4} = a_4 - R^{-1}B_3(B_3P_{34} + B_4P_{44})$$

$$b_{c1} = b_1 - R^{-1}B_3(B_3P_{31} + B_4P_{41})\,, b_{c2} = b_2 - R^{-1}B_3(B_3P_{32} + B_4P_{42})$$

$$b_{c3} = b_3 - R^{-1}B_3(B_3P_{33} + B_4P_{43})\,, b_{c4} = b_4 - R^{-1}B_3(B_3P_{34} + B_4P_{44})$$

The expression of ai (i=l,2,3,4), bi (i=2,4), F(X,r), B3 and B4 are equivalence to Equation (3.4) and Eq. (3.25) can be wrote as shown below:

$$\dot{X} = (A - BK)X + F(X,\tau)$$

After that, numerical simulation is conducted based on Eq. (3.25) and the structure of controlled system

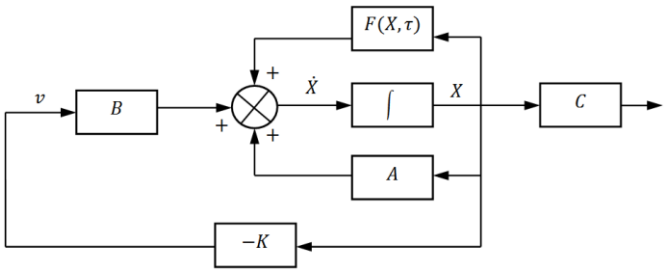

Figure 3.2 Structure of controlled system

The initial value of system state is $x_1(0) = 0.01, x_2(0) = x_3(0)x_4 = (0)$

4.1.piezoelectric chip length

Figure 4.1 showed the interaction between piezoelectric chip length and objective function J, with weights Q=I(I is unit matrix) , R=0.1, the distance between the top of piezoelectric sheets and pipes conveying fluid $\xi_a = 0$.

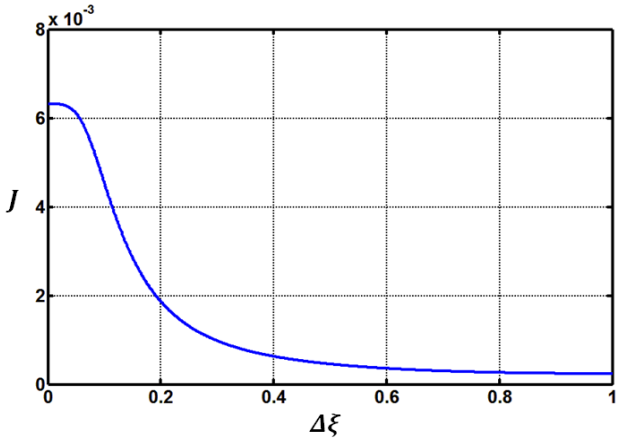

Figure 4.1 The objective function of pipes conveying fluid with the changes of piezoelectric sheets.

For pinned at both ends of pipes conveying fluid, the objective function J reaches a maximum when piezoelectric chip length Δξ=0.1, and a minimum when piezoelectric chip length Δξ=1. Figure 4.2 showed the relation among piezoelectric chip length, displacement response η and control input v. In comparison, at piezoelectric chip length Δξ = 0.6, pinned pipes conveying fluid systems tend to stability shortly and need less control inputs and small peak voltage. These are consistent with the result of objective function curve analysis.

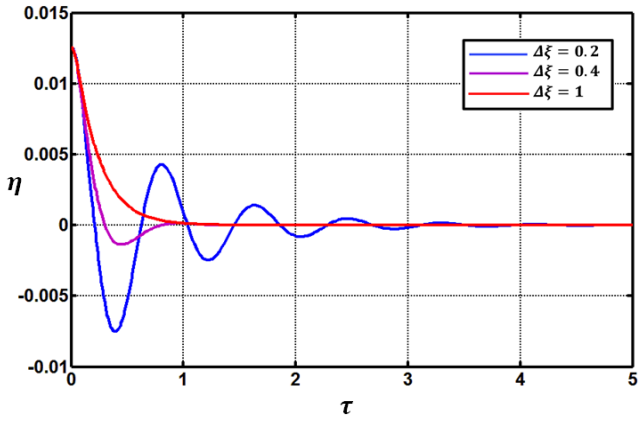

Figure 4.2(a) Displacement response curve of pipes conveying fluid at different piezoelectric chip length.

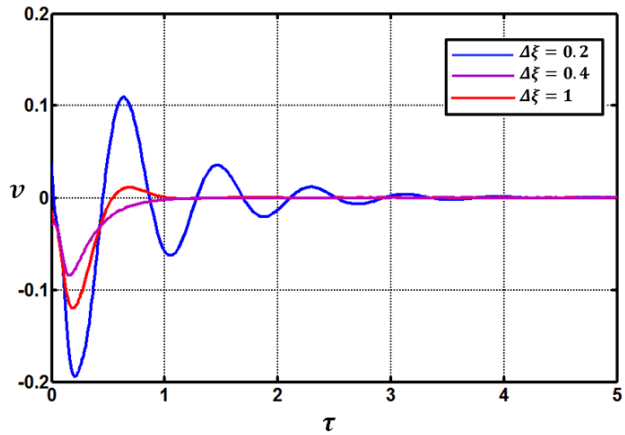

Figure 4.2 (b) Control input curves of pipes conveying fluid at different piezoelectric chip length.

4.2. Impact of the position of the piezoelectric

Figure 4.3 indicates the impact of the position of the piezoelectric on the objective function J with weights matrix Q=I, R=0.1; For pinned at both ends of pipes conveying fluid, piezoelectric chip length Δξ=0.2 is selected For pinned at both ends of pipes conveying fluid, J reaches a maximum when piezoelectric chip position $\xi_a = 0.8$, and a minimum when piezoelectric chip position $\xi_a = 0.402$ .. Figure 4.4 showed the impact of piezoelectric chip position to displacement response η and control input v.

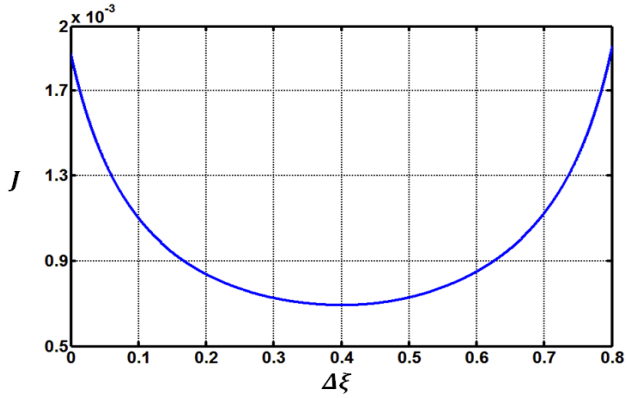

Figure 4.3 Objective function of pipe conveying fluid at different piezoelectric chip position.

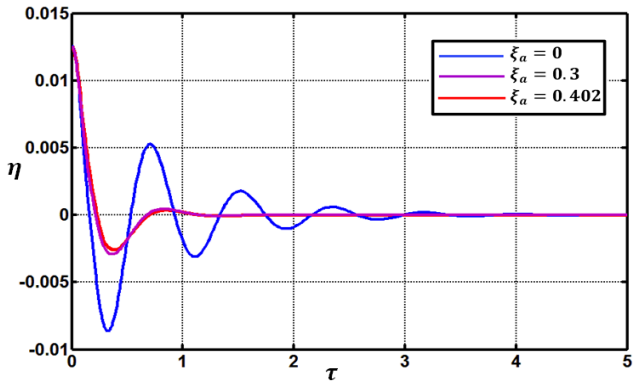

Figure 4.4 (a) Displacement response curve of pipe conveying fluid at different piezoelectric chip position.

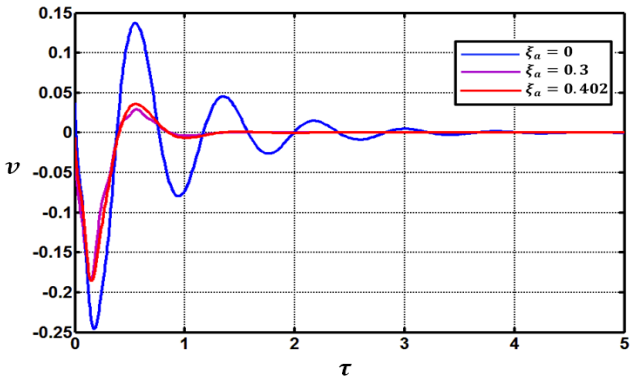

Figure 4.4 (b) Control input curve of pipe conveying fluid at different piezoelectric chip position.

In comparison, the control effect of pinned at both ends of pipes is basically the same as control input when $\xi_a = 0.3$ and 0.403, peak voltage is smaller when $\xi_a = 0.3$. These are in accordance with the result of objective function curve analysis

4.3. Selection of weighted value

According to Eq. (3.9), control system performance are highly dependent on selection of weight matrix Q and weight coefficient R .Control input and effect are able to be changed by adjusting Q and R. Figure 4.5 and 4.6 demonstrate the impacts of weight to the control effect and input of pinned at both ends of pipes. Suppose $Q = qI, \Delta\xi = 0.2, \xi_a = 0.3$

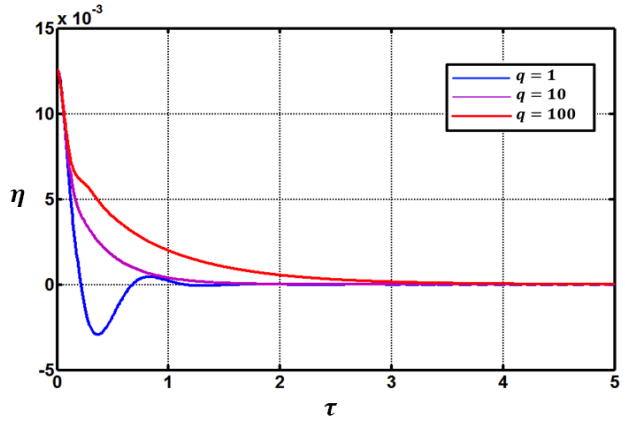

Figure 4.5 (a) The impact of control effect by weight matrix Q of pipes conveying fluid.

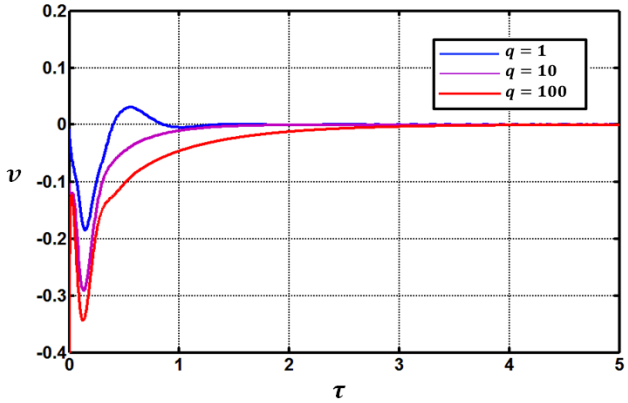

Figure 4.5 (b) The impact of control input by weight matrix Q pipes conveying fluid.

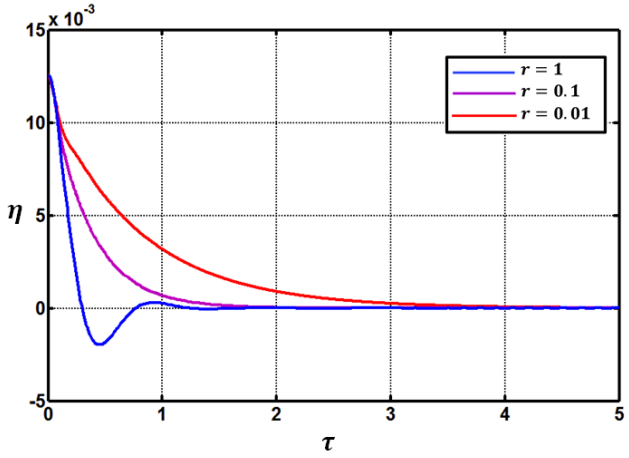

Figure 4.6 (a) The impact of control effect by weight matrix R of pipes conveying fluid.

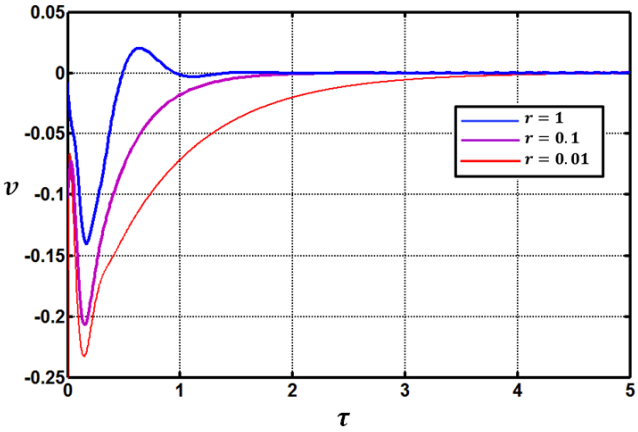

Figure 4.6 (b) The impact of control input by weight matrix R pipes conveying fluid.

Obviously, this system has achieved good control effect when R=0.1, Q=10I. Research indicates that the control input of system will increase if increasing weight matrix Q or decreasing weight coefficient R. While, it does not mean that the more control input, the better control effect. Actually, an optimal value is existed around weight value R=0.1, Q=10I.

This optimal value is not necessary in system control because this system has already had the ability to achieve a good control effects before reaching the best weight value, also at this time the control inputs and peak voltage are much smaller then selecting optimal value. In addition, it can be seen that weight matrix Q and weight coefficient R have the same impacts.

4.4 Effect of flow velocity

In controller design, u0=1.88 is designed for pinned and at both ends of pipes. Figure 4.7 demonstrate the control effects of average velocity at the first mode resonance of pinned at both ends of pipes, and we noted that the control system performance are highly dependent on flow velocity , its can reach good effect when average velocity increasing between 0 and

critical velocity (pinned at both ends of pipes u_{cr} =π).when the flow velocity increase ,the coriolis force and damping will increasing ,this lead to increasing the performance of the controller system.

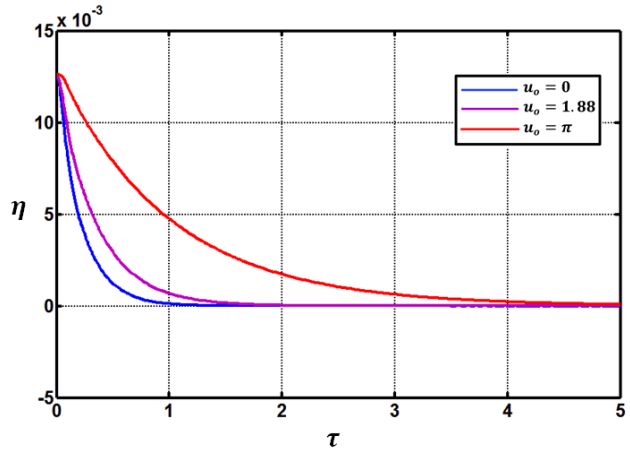

Figure 4.7(a) Displacement response curve of pipes conveying fluid at different flow velocity.

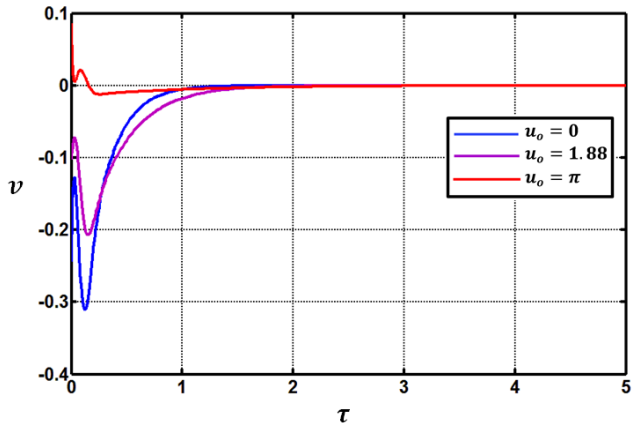

Figure 4.7 (b) Control input curves of pipes conveying fluid different flow velocity.

References

[1]- Lin Y H, Chu C L. Active flutter control of a cantilever tube conveying fluid using piezoelectric actuators. Journal of Sound and Vibration,1996,l96(l):97-105.

[2]- Tsai Y K, Lin Y H. Adaptive modal vibration control of a fluid-conveying cantilever pipe. Journal of Sound and Vibration, 1997,11 :535-547.

[3]- You C I-I, Bajaj A K., Nwokah O D l. Active control of chaotic vibration in a constrained flexible pipe conveying fluid. Journal of Fluids and Structures, 1995,9139-I22

[4]- Lin Yih I-Iwang, Huang Rui Chang, CItu Chih Liang. Optimal modal vibration suppression of a fluid-conveying pipe with a divergent mode. Journal of Sound and Vibration, 2l)04,27l ;577-597

[5]- Baz A, Poh S. Experimental implementation of the modified independent modal space control method. Journal of sound and Vibration. l990,l39(l):l33-149

[6]- Baz A, Poh S. Experimental implementation of the modified independent modal space control method. Journal of sound and Vibration. l990,l39(l):l33-149

[7]- Lin O R, Lin Z X, Z. L Wang. Cylindrical panel noise control using a pair of piezoelectric actuator and sensor. Journal of Sound and Vibration, 200i ,246(3):5Z5-541

[8]- Trindade M A, Benjedou A, Ohayon R, Piezoelectric active vibration control of damped sandwich beams. Journal of Sound and Vibration, 200l,246(4):653-677

[9]- Wang D, Wang C M, A controllability index for optimal design of piezoelectric actuators in vibration control of beam structures. Journal of Sound and Vtbration,2001,242(3):507-518

[10]- Zhou Y H, Wang J, Zheng X J, Vibration control of variable thickness plates with piezoelectric sensors and actuators based on wavelet theory. Journal of Sound and Vibration,2(100,237(3):395-410